Reducing Multipath Effect of Low-Cost GNSS Receivers for Monitoring by Considering Temporal Correlations

Li Zhang, Volker Schwieger

Institute of Engineering Geodesy University of Stuttgart, Geschwister-Scholl-Str. 24 D, 70174 Stuttgart, Germany (li.zhang@iigs.uni-stuttgart.de, volker.schwieger@iigs.uni-stuttgart.de)

Key words: *Low-cost GNSS; multipath-effect; temporal correlations analysis; monitoring*

ABSTRACT

The investigations on low-cost single frequency GNSS receivers at the Institute of Engineering Geodesy (IIGS) show that u-blox GNSS receivers combined with low-cost antennas and self-constructed L1-optimized choke rings can reach an accuracy which almost meets the requirements of geodetic applications (see Zhang and Schwieger, 2017). However, the quality (accuracy and reliability) of low-cost GPS receiver data should still be improved, particularly in environments with obstructions. The multipath effects are a major error source for the short baselines. The ground plate or the choke ring ground plane can reduce the multipath signals from the horizontal reflector (e.g. ground). However, the shieldings cannot reduce the multipath signals from the vertical reflectors (e.g. walls).

Because multipath effects are spatially and temporally correlated, an algorithm is developed for reducing the multipath effect by considering the spatial corrections of the adjoined stations (see Zhang and Schwieger, 2016). In this paper, an algorithm based on the temporal correlation will be introduced. The developed algorithm is based on the coordinates not on carrier phase raw data, which is easy to use. Because, for the users, coordinates are more accessible than the raw data. So that the algorithm is un The multipath effect can cause periodic oscillations but the periods change over time. Besides this, the multipath effect's influence on the coordinates is a mixture of different multipath signals from different satellites and different reflectors. These two properties will be used to reduce the multipath effect. The algorithm runs in two steps and iteratively. Test measurements were carried out in a multipath intensive environment; the accuracies of the measurements are improved by about 50% and the results can be delivered in near-real-time (in ca. 30 minutes), therefore the algorithm is suitable for structural health monitoring applications.

I. INTRODUCTION

Monitoring of artificial structures and natural objects is one of the main tasks of engineering geodesy. Low-cost single-frequency GNSS receivers are a cost-effective solution compared to traditional geodetic multi-frequency GNSS receivers, particularly for geodetic monitoring tasks where a high number of receivers are used. Numerous preliminary investigations have shown that low-cost single-frequency GPS receivers can achieve comparable results to geodetic GNSS receivers, if the carrier phase measurements of the GNSS receivers are evaluated for short baselines (Schwieger and Gläser, 2005; Schwieger, 2007; Schwieger, 2008; Schwieger, 2009; Limpach, 2009; Glabsch *et al.,* 2010). The influences of baseline-length-dependent errors, such as ionospheric and tropospheric errors, can be mitigated for short baselines. However, the site-dependent errors, such as the multipath effects, particularly in environments with obstructions, are the dominant errors of short baselines. In practice, very often the observation points for GNSS measurements are rarely selectable; e.g. for the monitoring of high buildings or television towers, there are normally many reflectors in the antenna vicinity.

Because the multipath effect is the dominant error in many applications, there has been a lot of research on the multipath effect since the beginning of GPS development. Many different methods have been developed to reduce the multipath effects by improving the hardware or algorithms (Van Dierendonck *et al.,* 1992; Axelrad *et al.,* 1994; Ray *et al.,* 1998; Choi *et al.,* 2004; Wanninger and May, 2000; Filippov *et al.,* 1998; Krantz *et al.,* 2001; Kunysz, 2003; Tatarnikov *et al.,* 2011). Because of the multipath effect complexity, there is no method which can completely eliminate the influence of the multipath effects up to now.

Moreover, many algorithms can only be used for post-processed measurements of static objects like reference stations, but they are not suitable for near-real-time kinematic monitoring applications. Furthermore, most of the algorithms are based on the carrier phase measurements which are not accessible to every user. The developed algorithm which will be introduced in this paper is based on the coordinates by considering temporal correlations, and the results will

be delivered in near-real-time, making this implementation suitable for structural health monitoring applications.

In section II, the relevant theoretical basis of the multipath effect will be given. The developed algorithm will be explained with an example in section III. The algorithm was evaluated with a lot of data; the test scenario, workflow and the results of the evaluation will be presented in section IV, followed by a short conclusion and outlook at the end of this paper.

II. Theoretical Basis of the Multipath Effect

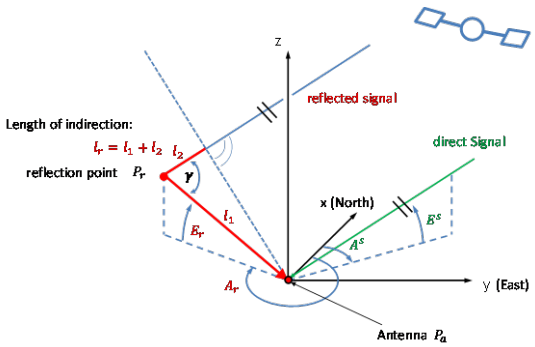

Figure 1. Geometric model of the multipath effect (after Irsigler, 2008)

As shown in Figure 1, the multipath effect is caused by a mixture of reflected and direct satellite signals, meaning that the received signal s_m is a combination of the reflected signal s_r and the direct signal s_d.

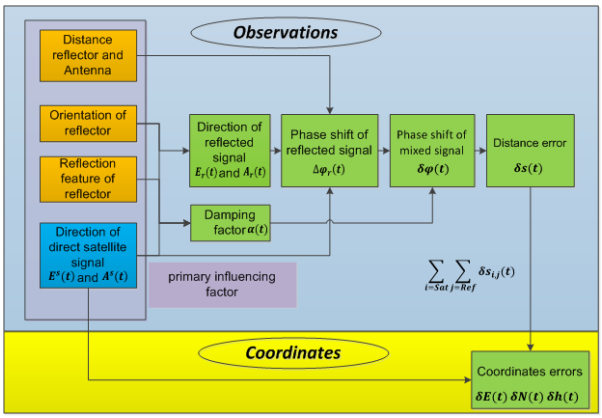

Figure 2. Overview of influencing factors of the multipath effect on coordinates

Figure 2 depicts the influencing factors of the multipath effect. The reflected signal has a longer way to reach the antenna (depending on the distance between reflector and antenna) and it loses some energy by reflection. So, the reflected signal has a phase shift $\Delta\varphi_r$ compared to the direct signal and a smaller amplitude A_r ($A_r = \alpha \cdot A_d$ with damping factor α) than that of the direct signal A_d. The damping factor α ($0 < \alpha < 1$) depends on the reflection feature of the reflector and the incidence angle of the reflected signals on the reflector (compare Figure 2). The incidence angle depends on the direction of the direct satellite signals $E^s(t)$ (elevation), $A^s(t)$ (Azimuth) and the orientation of the reflector. These different influencing factors are summarized as primary influencing factors in Figure 2.

Because $E^s(t)$ and $A^s(t)$ of satellites change over time, the multipath effect is not constant but temporally correlated.

In practice, it is difficult to get a value of the damping factor α, because it changes over time and it changes also with the inclination angle of the satellite signal. The damping factor α changes even with the reflection feature of the reflector; e.g. Wanninger and May (2000) describe the phenomenon that the multipath effects at the reference stations change when it snows.

The multipath effect can cause periodic oscillations (Georgiadou and Kleusberg, 1988) on the carrier phase measurement and the periodic effect can also be found in the coordinates (Heister *et al.*, 1997). Their relationship is shown in Figure 2 and will be discussed later on in this contribution.

The so-called multipath frequency on the carrier phase for the horizontal and vertical reflectors can be estimated using the equation (1) (Irsigler, 2008):

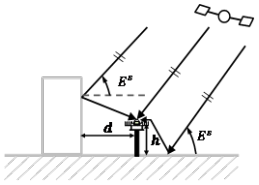

Figure 3. Reflection of the satellite signals on horizontal and vertical reflector

$$f_{\delta\varphi}(t) = \frac{2}{\lambda} \cdot \begin{cases} h \cdot \cos E^s(t) \cdot \dot{E}^s(t) & \text{horizontal} \\ -d \cdot \sin E^s(t) \cdot \dot{E}^s(t) & \text{vertical} \end{cases} \quad (1)$$

where λ is the wavelength, h and d are the vertical and horizontal distances between the antenna and the reflector (compare Figure 3). The closer the reflector is located to the antenna, the longer the period.

$E^s(t)$ and $\dot{E}^s(t)$ are the satellite elevation and its velocity. Because they are varying in time, the multipath frequencies also change over time.

Equation (1) shows the fact that the multipath frequencies are independent of the damping factor α .

Generally, in practice there are more reflectors with different orientations in the antenna vicinity, thus the multipath effect on coordinates is generally a mixture of several reflected signals. This means that one direct signal could be reflected by several reflectors and one reflector could reflect several satellite signals.

For example, the phase error of mixture signal $\delta\varphi_{i,j}(t)$ from satellite i and reflector j can be calculated in a distance error by equation (2):

$$\delta s_{i,j}(t) = \delta\varphi_{i,j}(t) \cdot \frac{\lambda}{\pi} \quad (2)$$

The influences of the reflected signal on the coordinates $\delta E_{ij}(t)$, $\delta N_{ij}(t)$, $\delta h_{ij}(t)$ from satellite i and reflector j is the projection of distance error $\delta s_{i,j}$ on the different coordinate components, and could be expressed by:

$$\begin{pmatrix} \delta E_{ij}(t) \\ \delta N_{ij}(t) \\ \delta h_{ij}(t) \end{pmatrix} = \delta s_{ij}(t) \cdot \begin{pmatrix} -\cos E_i^s(t) \cdot \cos A_i^s(t) \\ \cos E_i^s(t) \cdot \sin A_i^s(t) \\ \sin E_i^s(t) \end{pmatrix} \quad (3)$$

Therefore, the multipath effect on the coordinates can be written as:

$$\begin{aligned} \delta E(t) &= \sum_{i=1}^{i=m} \sum_{j=1}^{j=n} \delta E_{i,j}(t) \\ \delta N(t) &= \sum_{i=1}^{i=m} \sum_{j=1}^{j=n} \delta N_{i,j}(t) \\ \delta h(t) &= \sum_{i=1}^{i=m} \sum_{j=1}^{j=n} \delta h_{i,j}(t) \end{aligned} \quad (4)$$

where m = number of satellites
n = number of reflectors

Considering equation (1), the multipath effect on the coordinates should be a combination of many periodic oscillations which are originated from the multipath effect on the carrier phases.

The basic idea of the estimation of the periodic oscillations in the multipath effect on the coordinates is to reduce the multipath effect. In the next section, the developed algorithm will be introduced.

III. ALGORITHMS

As described in section II, the multipath effect on the coordinates x_i could be regarded as a combination of several periodic oscillations:

$$x_i = \sum_{j=1}^{q} x_j \quad (5)$$

where i:= 1, 2, 3 (3 coordinate components)
j:= 1 to q (q periodic oscillation caused by multipath effect)

The periodic oscillations can be illustrated as:

$$x_j = A_j \cdot sin\left(2\pi f_{\delta\varphi,j} t_i + \Delta\varphi_j\right) \quad (6)$$

where $f_{\delta\varphi,j}$:= j-th multipath frequency
A_j:= corresponding amplitude
$\Delta\varphi_j$:= corresponding phase shift

The disadvantage of the equation (6) is that the function is not linear and the approximated value of amplitude and phase shift should be known so that they could be estimated by adjustment. Thus, the equation (6) will be restated to:

$$x_j = a_j \cdot sin\left(2\pi f_{\delta\varphi,j} t_i\right) + b_j \cdot cos\left(2\pi f_{\delta\varphi,j} t_i\right) \quad (7)$$

where $a_j = A_j \cdot cos\,\Delta\varphi_j$

$b_j = A_j \cdot sin\,\Delta\varphi_j$

So, if the multipath frequency $f_{\delta\varphi,j}$ is given, the parameters a_j and b_j could be estimated by linear adjustment. The estimated x_j could be subtracted iteratively from the coordinates in order to eliminate the multipath effect from the coordinates.

A. *Search Process*

One way to get the multipath frequency is to get it from the periodogram. The disadvantage is that the spectral resolution of the periodogram is limited (see example in section III.C). In order to increase the spectral resolution, the multipath frequency $f_{\delta\varphi,j}$ is at first roughly estimated from the periodogram and then precisely estimated in a so-called search process by adjustment; this means $f_{\delta\varphi,j}$ will be estimated in two steps.

Step 1: If the periodogram has a maximum at j-th iteration (it is the j-th multipath frequency) at the frequency of $f_k = k \cdot \Delta f$, where Δf is the resolution of periodogram and k is the corresponding index of the frequency f_k, then f_k will be taken for further analysis in step 2.

Step 2: The multipath frequency $f_{\delta\varphi,j}$ can be searched between the $f_{k-1} = (k-1) \cdot \Delta f$ and $f_{k+1} = (k+1) \cdot \Delta f$. That means the multipath period $T_{\delta\varphi,j}$ can be searched between $T_{k+1} = 1/f_{k+1}$ and $T_{k-1} = 1/f_{k-1}$. For the search process, one so-called search interval ΔT should be defined, e.g. $\Delta T =$ 1 second. Afterwards all the periods between T_{k+1} and T_{k-1} (with search interval ΔT) will be taken in the adjustment. The period with the sum of squared residuals is the optimum. In this way, the precise multipath period $T_{\delta\varphi,j}$ or multipath frequency $f_{\delta\varphi,j}$ in the j-iteration is estimated.

B. *Remarks*

Remark 1: Significance tests should be done for estimated parameters a_j and b_j in every iteration. As the phase shift $\Delta\varphi_j$ could be nearby 0°, 90°, 180°, 270° or 360°, the parameters a_j and b_j could be nearby zero. So at least one of these two parameters should be significant in t-distribution. This means that they are tested separately. Besides, the parameters a_j and b_j belong to the same frequency $f_{\delta\varphi,j}$, so that they can be regarded as tuple. For this reason, their significance is also tested together by using the χ^2-distribution, where the correlation between the two parameters a_j and b_j is considered (more details can be found in Zhang, 2016).

Remark 2: The estimated multipath period $T_{\delta\varphi,j}$ can be regarded as mean value for the defined time block. The multipath period $T_{\delta\varphi,j}$ is temporally variable and not constant (compare section II).

Remark 3: Although the sampling rate is e.g. 1 second, the estimated multipath period $T_{\delta\varphi,j}$ should not be an integer value. This is because, as mentioned

in Remark 2, the estimated multipath period $T_{\delta\varphi,j}$ is a mean value for a defined time block. For this reason, the search interval ΔT could be defined as any float number, e.g. ΔT = 0.1 second or ΔT = 0.01 second. The estimated multipath period $T_{\delta\varphi,j}$ can be even more precise, so that the residuals after the adjustment could be even smaller. The problem is that an optimum result will then require much more time. So some compromise should be found between better results and less calculation time.

Remark 4: If a high amplitude is shown at the index k = 1 in the periodogram, it means that the time series contains trends and it is not stationary. In this case, it is possible that the coordinate time series is influenced by long-period multipath effects. For the search process this means that the multipath period $T_{\delta\varphi,j}$ should be searched between $T_0 = \infty$ (or $f_0 = 0$) and $T_2 = 1/(2 \cdot \Delta f)$. However, it is not appropriate to estimate a long-period wave from a short observation time. Empirically, at least half of the wave should be within the observation time, so that the period could be estimated. For example, if the observation time is 3600 seconds, the maximum of the estimated period is 7200 seconds.

C. *Example*

To explain the developed algorithm, the residuals of the height component of one baseline (1 hour) are taken as an example.

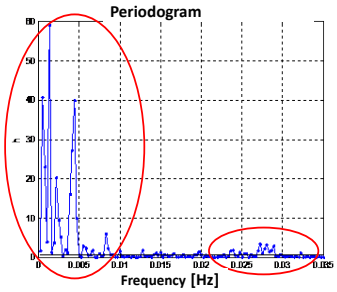

Figure 4. Periodogram of the height component

In Figure 4, high amplitudes are shown at several frequencies, which again indicates the fact that the multipath effect on the coordinates is the mixture of several multipath signals influences. Here, high values of the periodogram are between 0.025 and 0.03 Hz, and 0 und 0.01 Hz (marked area in Figure 4).

Table 1. Interpretation of periods

Index k	Period T_k [s]
1	3600
2	1800
3	1200
4	900
5	720

The spectral resolution of the periodogram depends on the observation time and sampling rate, here the observation time is 3600 seconds and the sampling rate is 1 second. So the spectral resolution is here Δf = 1/3600 Hz. Table 1 shows, as examples, the periods for the first five indices in the periodogram. It is obvious that the spectral resolution is low, especially if the frequency is close to zero.

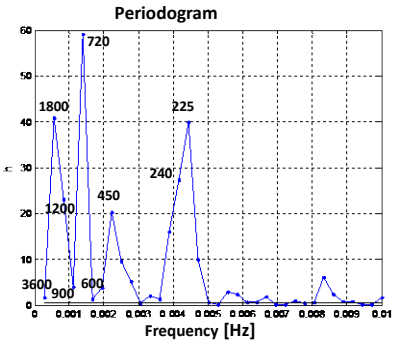

Figure 5. Periodogram with interpretation of periods

Figure 5 shows periods of several frequencies/indices with high amplitudes. For example, the period of index k =2, 5 or 16 is T_k = 1800, 720 or 225 seconds.

For the first iteration (j = 1), the maximum amplitude is at T_5 = 720 seconds. The multipath period in the first iteration will then be searched in neighborhood of T_5, it means between T_6 = 600 seconds and T_4 = 900 seconds. A search interval ΔT = 1 second is taken for the search process. So, every integral value between 600 and 900 seconds will be taken as potential multipath frequency in equation (7) and the sum of squared residuals can be calculated.

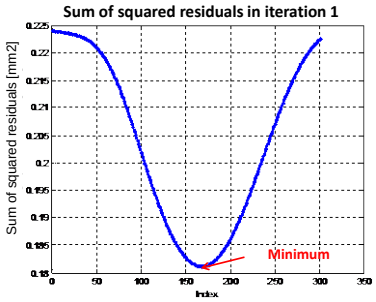

Figure 6. Sum of squared residuals of search process in iteration 1

Figure 6 shows the sum of squared residuals in the first iteration. The minimum of the sum of squared residuals is at index 167. That means the precise multipath period in the first iteration $T_{\delta\varphi,1}$ is 767 seconds ($600 + 167 \cdot \Delta T$). And after that the periodic oscillation with $T_{\delta\varphi,1}$ will be eliminated from the residuals. This procedure will run until only white noise is remaining or the parameters a_j and b_j are not significant any more. In this example, 14 iterations are needed.

Figure 7 shows a comparison of original residuals (with +40 mm offset for better comparison or visualization) and the residuals after using the developed algorithm. It is clearly observable that the periodic oscillations in the original residuals are significantly reduced by applying the developed algorithm. The standard deviation is improved by 43% (from 7.9 mm to 4.5 mm).

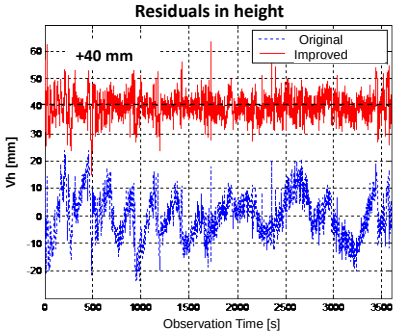

Figure 7. Comparison of residuals

Figure 8 shows a periodogram of the original residuals and of the residuals after using the algorithm with precise frequency. Some of the found precise multipath periods are also shown in Figure 8. This indicates the same effect as Figure 7, that the developed algorithm reduces the periodic oscillations in the original residuals.

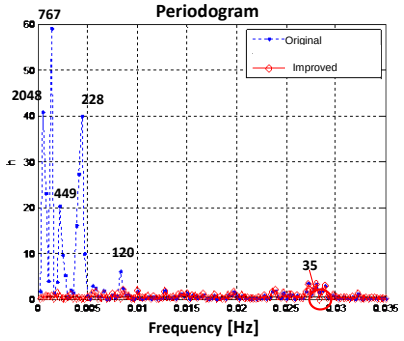

Figure 8. Comparison of periodogram with precise frequency

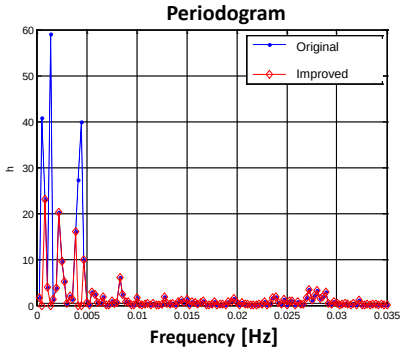

Figure 9. Comparison of periodogram without precise frequency

For the case that the periods from the periodogram are directly used (e.g. T_5 = 720 is directly used in the first iteration), the results are shown in Figure 9. It can be seen that amplitudes of some frequencies are reduced, however, not as much as in Figure 8 (with precise frequencies). The standard deviation is improved only by 19% (from 7.9 mm to 6.4 mm).

IV. Evaluation

A. *Test Scenario*

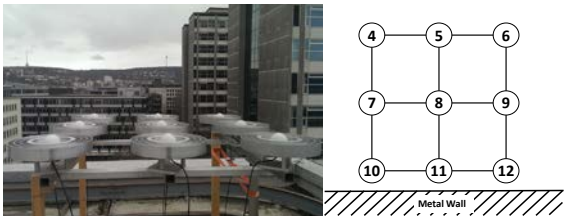

Figure 10. Photos of test field with antenna array and antenna number

For evaluation of the developed algorithm, a large data set was used. As shown in Figure 10, a 3 × 3 antenna array was set up next to the metal wall on the roof of the IIGS-building, with a 0.5 m distance between antennas. U-blox LEA-6T GPS receivers are combined with Trimble Bullet III GPS antennas (cost about 100 €) and the self-constructed L1-optimized choke ring ground plane.

The choke ring ground plane can reduce the influence of the reflected signal coming from the ground but they cannot prevent the antennas from the reflected signals which are higher than the antenna horizon (Weill, 1997). The test results in Zhang and Schwieger (2017) have proved this fact. In this test field, most multipath signals are from the metal walls in antenna vicinity, not from the ground.

Static measurement has been undertaken for 26 days in the spring of 2014. The GPS raw data were recorded from the 9 receivers at 1 Hz, stored on a PC, evaluated and post-processed. One SAPOS reference station (Satellitenpositionierungsdienst der Deutschen Landesvermessung; English: German Satellite Positioning Service) is only about 500 m away from the test field. This station is taken as reference station and the 9 stations in the test field are taken as rover stations for processing the baselines so that 9 baselines can be calculated.

The raw data of the 9 stations are in UBX binary format and are converted into RINEX format using the TEQC (TEQC, 2014) provided by Unavco (Unavco, 2014) and the baseline is processed by software Wa1 provided by Wasoft (Wasoft, 2015). The results of Wa1 are the baselines in the UTM-Coordinate System in east, north and height for every second. The outliers in the coordinate's time series, which are probably caused by unfixed ambiguities, are detected according to the 3σ-rule and linearly interpolated. Finally, the standard deviation is calculated.

B. *Evaluation Workflow*

The antenna array in the test field is used to analyze the spatial correction of the antennas. One algorithm is developed to reduce the multipath effect using the spatial corrections and published in Zhang and Schwieger (2016), where two antennas are needed. The described algorithm in this paper is based on the temporal correlation and needs only one station to reduce the multipath effect.

One day data is taken to test the performance of this described algorithm based on temporal correlation. Figure 11 shows the workflow of the evaluation. Temporal correlations of the coordinate series in this test are not significant after about 15 minutes (see the analysis in Zhang and Schwieger, 2016) and in order to simulate the near-real-time solution, one day coordinates residuals were divided into 96 15-minutes blocks (900 seconds). Since there is no deformation during the measurement, a step deformation (with 1σ) is simulated in the middle of the first block (at 450th second). For the baseline s-a4 (antenna number 4), σ_E = 3.2 mm, σ_N = 5.6 mm and σ_h = 9.0 mm (from daily solution) are taken as σ values for the step deformation for each coordinate component.

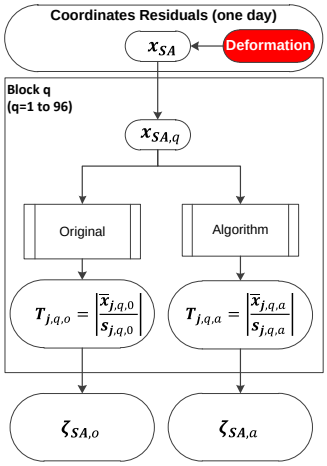

Figure 11. Evaluation workflow

For the deformation analysis, the standard deviation and mean value for each block is calculated, and the mean value may be tested for the significance by equation (8):

$$T_{j,q} = \left|\frac{\bar{x}_{j,q}}{s_{j,q}}\right| \sim t_{f,97.5\%}. \qquad (8)$$

where j:= 1 to 3 (3 coordinate components)
q:= 1 to 96 (96 blocks)

If the test value $T_{j,q}$ exceeds for example the quantile $t_{f,97.5\%}$ (t-distribution), a deformation is detected. Since the number of observations is large, the Gaussian distribution is assumed to be an approximation of the t-distribution. The developed algorithm can decrease the standard deviations so that Detection quota of deformation ζ is increased.

C. *Evaluation Results*

Figure 12 shows the difference of the 3D-position standard deviation of the 96 blocks (baseline s-a4). The standard deviation is improved by 51% (from 9.1 mm to 4.5 mm). It leads to the increase of the mean detection quota of 1σ deformation of 40% (compare Table 2).

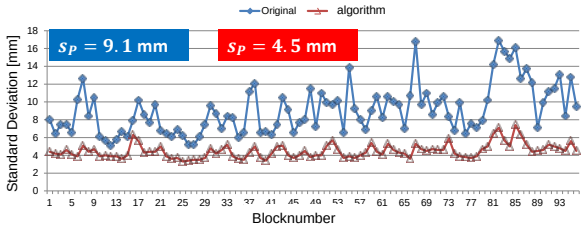

Figure 12. Comparison of standard deviations of blocks

Table 2. Detection quota of 1σ deformation

	ζ_E	ζ_N	ζ_h	ζ_m
Original	5.2%	13.5%	8.3%	9.0%
Algorithm	42.7%	55.2%	47.9%	48.6%

The evaluation was done by all the 9 baselines. In average, the 3D-position standard deviations and the detection quotas of 1σ deformation are improved by 52% and 47.6% respectively. The developed algorithm was also used to reduce the multipath effect in the monitoring of a church tower (see Zhang et al, 2018), the standard deviation is improved by about 45%.

Furthermore, it should be noted that the deformation detection sensitivity is increased through the developed algorithm. However, the probability of a false alarm is also increased. That is because this algorithm can only reduce oscillations within short periods (up to double of block length). Some multipath effects cause oscillations with long periods. Actual step or linear deformations will be kept in the following coordinate time series. In contrast, the long periodic oscillation coordinates behavior is elastic. If deformation is detected in two successive blocks, it can then be finally defined as deformation. In this way to probability of a false alarm could be reduced (from 12.8% to 1.3%, more details can be found in Zhang, 2016). In such a case, reliable results can be delivered in near real-time with a delay of 30 minutes.

V. CONCLUSION AND OUTLOOK

In this paper, the theoretical basis of the multipath effect is presented. The influencing factors of the multipath effect were introduced. The temporal correlation of the multipath effect and the relationship of the multipath effect on the carrier phase and the coordinates is discussed and explained. Based on the theory, the developed algorithm that takes temporal

correlation of the coordinates into consideration, is explained by an example. The multipath frequencies can be precisely and iteratively estimated, so that the periodic oscillations caused by the multipath effects can be reduced on the coordinate residuals. As a result, the standard deviation of the measurement can be significantly improved by about 50%. In case of monitoring applications with step and linear deformation, the algorithm can help to detect the deformation more quickly and reliably. The improvement of the probability for detection of a deformation of 1σ is about 40%. A reliable detection in 30 minutes is possible.

The estimation of the precise multipath frequencies can be optimized in the future. For example, the optimal period could be searched starting with a big search interval (e.g. every 10 seconds) and finally with a smaller interval nearby the precise frequency (e.g. every 1 second or even shorter, e.g. 0.1 second), so that the algorithm could run more quickly and the results could be even more precise.

Thus this paper shows the possibility of the low-cost GPS antenna with the temporal correlation based algorithm for the structural health monitoring applications, particularly in the case of high multipath effects. In the future, the algorithm should be evaluated and improved for real monitoring objects like landslide, and the method should be adapted if it is applied for the monitoring of buildings and bridges with periodic deformations. If the frequency of the periodic deformation is known, one possibility might be considering this in the coordinates, so that it will not be eliminated by the developed algorithm. This approach should be tested in the future. Furthermore, the correlation between the coordinates' components should also be investigated in the future.

References

Axelrad, P., C. Comp, and P. MacDoran (1994). Use of Signal-To-Noise Ratio for Multipath Error Correction in GPS Differential Phase Measurements: Methodology and Experimental Results. In: Proceedings of the 7th International Technical Meeting of the Satellite Division of the Institute of Navigation, Salt Lake City, pp. 655-666.

Choi, K., A. Bilich, K. M. Larson, and P. Axelrad (2004). Modified sidereal filtering: Implications for high-rate GPS positioning. Geophysical Research Letters, doi: 10.1029/2004GL021621.

Filippov, V., D. Tatarnicov, J. Ashjaee, A. Astakhov, and I. Sutiagin (1998). The First Dual-Depth Dual-Frequency Choke Ring. In: Proceedings of the 11th International Technical Meeting of the Satellite Division of The Institute of Navigation, Nashville.

Georgiadou, Y, and A. Kleusberg (1988). On Carrier Signal Multipath Effects in relative GPS Positioning. Manuscripta Geodaetica, Band 13, pp. 172-199.

Glabsch, J., O. Heunecke, S. Pink, and S. Schubäck (2010). Nutzung von Low-Cost GNSS Empfängern für ingenieurgeodätische Überwachungsaufgaben. In: GNSS 2010 - Vermessung und Navigation im 21. Jahrhundert. DVW-Schriftenreihe, Band 63, Wißner-Verlag, Augsburg, pp. 113-129.

Heister, H., R. Hollmann, and M. Lang (1997). Multipath-Einfluß bei GPS-Phasenmessungen: Auswirkungen und Konsequenzen für praktische Messungen. In: AVN, Band 5, pp. 166-177.

Irsigler, M. (2008). Multipath Propagation, Mitigation and Monitoring in the Light of Galileo and the Modernized GPS. Dissertation, Bundeswehr University Munich.

Krantz, E., S. Riley, and P. Large (2001). The Design and Performance of the Zephyr Geodetic Antenna. In: Proceedings of the 14th International Technical Meeting of the Satellite Division of The Institute of Navigation, Salt Lake City, pp. 11-14.

Kunysz, W. (2003). A Three Dimensional Choke Ring Ground Plane Antenna. In: Proceedings of the 16th International Technical Meeting of the Satellite Division of the Institute of Navigation, Portland, pp. 1883-1888.

Limpach, P. (2009). Rock glacier monitoring with low-cost GPS: Case study at Dirru glacier, Mattertal. AHORN, Zurich.

Ray, J. K., M. E. Cannon, and P. Fenton (1998). Mitigation of Static Carrier Phase Multipath Effects Using Multiple Closely-Spaced Antennas. In: Proceedings of the 11th International Technical Meeting of the Satellite Division of the Institute of Navigation, Nashville, pp. 1025-1034.

Schwieger, V. (2007). High-Sensitivity GNSS - the Low-Cost Future of GPS?. In: Proceedings on FIG Working Week, Hongkong.

Schwieger, V. (2008). High-Sensitivity GPS - an availability, reliability and accuracy test. In: Proceedings on FIG Working Week, Stockholm.

Schwieger, V. (2009). Accurate High-Sensitivity GPS for Short Baselines. In: Proceedings on FIG Working Week, Eilat.

Schwieger, V., and A. Gläser (2005). Possibilities of Low Cost GPS Technology for Precise Geodetic Applications. In: Proceedings on FIG Working Week, Kairo.

Tatarnikov, D., A. Astakhov, and A. Stepanenko (2011). Convex GNSS Reference Station Antenna. In: Proceeding of International Conference on Multimedia Technology (ICMT), Hangzhou, pp. 6288-6291.

TEQC (2014). http://facility.unavco.org/software/teqc/teqc.html. Last Access: 30.02.2014.

Unavco (2014). https://www.unavco.org. Last Access: 23.11.2014.

Van Dierendonck, A. J., P. Fenton, and T. Ford (1992). Theory and Performance of Narrow Correlator Spacing in a GPS Receiver. In: Navigation: Journal of the Institute of Navigation, Volume 39, Issue 3, pp. 265-283.

Wanninger, L., and May, M. (2000). Carrier Phase Multipath Calibration of GPS Reference Stations. In: Proceedings of ION GPS 2000, Salt Lake City, pp. 132-144.

Wasoft (2015). http://www.wasoft.de/. Last Access: 23.09.2015.

Weill, L. R. (1997). Conquering Multipath: The GPS Accuracy Battle. In: GPS World, Volume 8, Issue 4, pp. 59-66.

Zhang, L., and V. Schwieger (2016). Improving the Quality of Low-Cost GPS Receiver Data for Monitoring Using Spatial Correlations. Journal of Applied Geodesy, 10(2): pp. 119-

129. ISSN (Online) 1862-9024, ISSN (Print) 1862-9016, DOI: https://doi.org/10.1515/jag-2015-0022.

Zhang, L., and V. Schwieger (2017). Investigation of a L1-optimized choke ring ground plane for a low-cost GPS receiver-system. Journal of Applied Geodesy, 12(1), pp. 55-64, 2017. ISSN (Online) 1862-9024, ISSN (Print) 1862-9016, DOI: https://doi.org/10.1515/jag-2017-0026.

Zhang, L. (2016). Qualitätssteigerung von Low-Cost-GPS Zeitreihen für Monitoring Applikationen durch zeitlich-räumliche Korrelationsanalyse, Dissertation at University of Stuttgart.

Zhang, L., I. Ionescu, and V. Schwieger (2018). Monitoring of the Church Tower in Herrenberg with Low-Cost GNSS. In: Proceeding of Geoprevi 2018 International Symposium, 29-30 October 2018, Bucharest, Romania.